ChemComm

Cite this: *Chem. Commun.*, 2012, **48**, 4884–4886

www.rsc.org/chemcomm

COMMUNICATION

Spirally configured *cis*-stilbene/fluorene hybrids as bipolar, organic sensitizers for solar cell applications†

Wei-Shan Chao,[a] Ken-Hsien Liao,[b] Chien-Tien Chen,*[b] Wei-Kai Huang,[c] Chi-Ming Lan[c] and Eric Wei-Guang Diau*[c]

Received 15th November 2011, Accepted 21st March 2012
DOI: 10.1039/c2cc17079e

Hybrids based on a dibenzosuberene core bearing a spiro-fluorene junction at the C-5 position and with amino donor and β-thiophenyl-α-cyanoacrylic acid acceptor groups at C-3 and C-7, respectively, serve as new organic sensitizer materials for solar cell applications. Solar cell devices based on these materials show a conversion efficiency (η) of up to 6.1% (V_{oc} = 697 mV, J_{sc} = 12.2 mA cm^{-2}, FF = 0.72) under AM 1.5 G conditions. The best IPCE values exceed 75% within the 450–550 nm absorption range.

The interest on dye-sensitised solar cells (DSSCs) began with the breakthrough made by Grätzel and co-workers[1] who have documented efficiencies of 11% with Ru/bi- or terpyridine-based sensitizers.[2,3] Conversely, DSSCs made of porphyrin and phthalocyanine dyes gradually catch up the leads.[4] Metal-free dyes bearing perylene, coumarin, or indoline core have also been used for DSSCs.[5] Some devices made of organic dyes employing an EDOT–dithienosilole linked spacer have reached a level of efficiency comparable to those of Ru dyes.[6] The structural design of an organic dye is often based on the donor–(π bridge)–acceptor (D–π–A) motif due to facile intramolecular charge transfer with evident bathochromic shift of the light absorption profiles.

In recent years, we have explored the utility of the dibenzosuberene (DBE) unit as a configurationally confined *cis*-stilbene (STI) template when spirally linked to fluorene at the C-5 position. The resulting hybrid (STIF) serves as a new type of optoelectronic template in organic light-emitting diode applications with great success.[7] We sought to extend its utility towards DSSC applications by appending amino donor (D) and β-thiophenyl-α-cyanoacrylic acid (TCA) acceptor groups at the C-3 and C-7 positions, respectively. Recently, notable power conversion efficiencies (η) of DSSC employing *trans* β-styryl (3.1–5.9%),[8] β-thiophenylstyryl (4.1–7.0%),[9] stilbenyl (4.6–9.1%),[10a,b] and fluorenylvinylene (5.6%)[10c] blocks as π-spacers for bipolar dyes have been reported. To date, the corresponding *cis*-stilbene variants have never been explored. In principle, the rigid spirally configured, *cis*-stilbene framework would impose a better π-conjugation. Therefore, the bipolar, DBE/spiro-fluorene hybrid assembly might have the advantages of increasing light absorptions for superior light harvesting, decreasing back electron transfer for better charge separation, and preventing approaching of I_3^- into the dye/TiO_2 interface for retarded charge recombination.

The target dyes **1–5** were obtained by a synthetic protocol illustrated in Scheme 1.[11] Hartwig coupling reaction was used to append five different arylamine groups at the C-3 position of the 3,7-dibromo-STIF.[7c] The resulting intermediates were subjected to Suzuki coupling reactions (72–80% yields) by treatment with 5-formylthiophene–boronic acid.[11] Subsequent condensation of the aldehyde intermediates with cyanoacetic acid in catalytic piperidine (10 mol%) provided the desired dyes **1–5** in 72–78% yields.[11]

The stacked absorption spectra of **D-STIF–TCA** dyes **1–5** and the unconstrained **2′** bearing a *cis*-stilbene core in THF solution and TiO_2 film are displayed in Fig. 1 and the corresponding data are shown in Table 1. In all cases except **4** (D = Fl_2N), two strong absorption bands with λ_{max} centered at 377 ± 3 nm and 455 ± 3 nm, respectively, were observed. The former band can be attributed to π–π* transitions, and the latter one to photoinduced, intramolecular charge transfer (PICT) from a given arylamine donor to α-cyanoacrylic acid

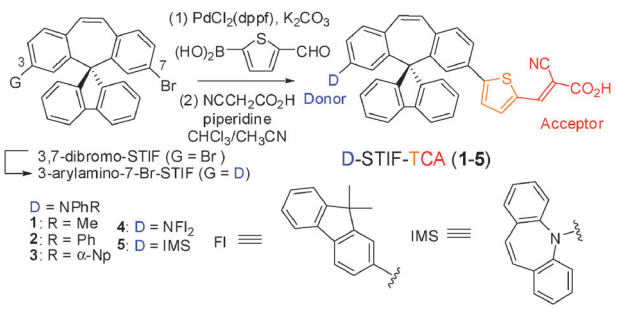

Scheme 1 The design and synthesis of **D-STIF–TCA** dyes.

[a] *Department of Chemistry, National Taiwan Normal University, #88, Sec. 4, Ding-jou Road, Taipei 11677, Taiwan*
[b] *Department of Chemistry, National Tsing Hua University, #101, Sec. 2, Kuang-Fu Rd., Hsinchu 30013, Taiwan. E-mail: ctchen@mx.nthu.edu.tw; Fax: +886-3-5711082; Tel: +886-3-5739240*
[c] *Department of Applied Chemistry and Institute of Molecular Science, National Chiao Tung University, 1001 University Rd., Hsinchu 30010, Taiwan. E-mail: diau@mail.nctu.edu.tw; Fax: +886-3-5723764; Tel: +886-3-5131524*

† Electronic supplementary information (ESI) available: Experimental procedures, characterization and NMR spectra for all compounds. CCDC 868581 and 871304. For ESI and crystallographic data in CIF or other electronic format see DOI: 10.1039/c2cc17079e

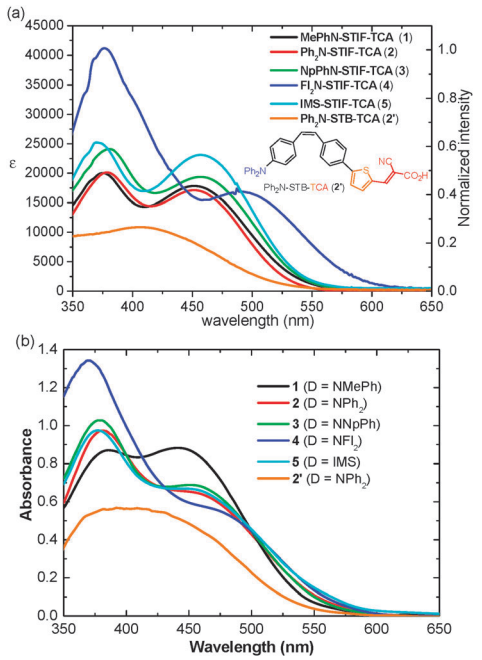

Fig. 1 Stacked absorption spectra of **1–5** in (a) THF and (b) TiO_2 film.

through conjugated STIF and thiophene linker. The PICT band is shifted to 492 nm in the case of **4** presumably due to enhanced conjugation. In marked contrast, **2′** exhibits a blue shift by 46 nm for the PICT absorption band with a dramatically reduced ε value by 57% (Fig. 1a). Moreover, the absorption spectrum of **2′** on film grows up in the shorter wavelength region and is much broader than that in solution, which indicates an H-type aggregation of **2′** on film.

The oxidation potentials (E_{ox}) of **D-STIF–TCA** dyes were obtained by cyclic voltammetry measurements. In all cases except **4** (E_{ox} = 0.36 eV), the oxidation potentials which are attributed to the oxidation of different arylamine moieties at C3 (Table 1) fall in the range of 0.52–0.63 eV. Their relative trend towards oxidation follows the order of **4** (D = Fl_2N) > **5** ≈ **1** ≈ **3** > **2** (D = NPh_2), indicating the strongest electron-donating nature of the Fl_2N group.[5d] The excited-state potentials [$E(S^+/S^*)$] of the dyes **1–5** (−1.78 to −2.02 V *vs.* NHE) were deduced from respective E_{ox} and zero–zero excitation energy (E_{0-0}) as calculated by the longest absorption band edge. Their [$E(S^+/S^*)$] are 1.2–1.5 V higher than the conduction band energy of the TiO_2 working electrode (−0.57 V *vs.* NHE), which secure electron injection from the photo-excited dyes into the TiO_2 electrode. Conversely, their $E(S^+/S)$ are 0.13–0.23 V lower than the chemical

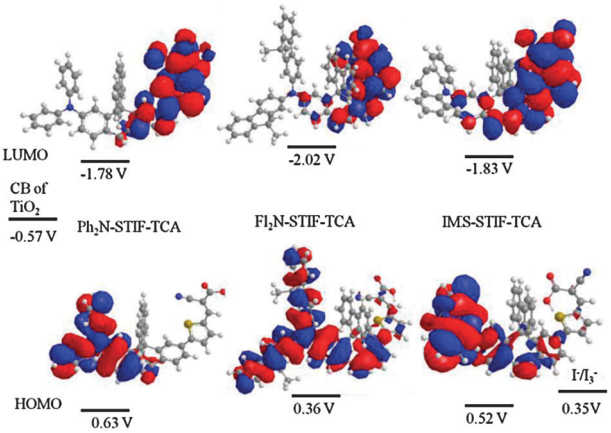

Fig. 2 The calculated frontier molecular orbitals of **Ph_2N-**, **Fl_2N-**, and **IMS-STIF–TCA** dyes.

potential of the I^-/I_3^- redox pair (+0.35 V *vs.* NHE), providing favourable conditions for hole transfer.

In addition, theoretical calculations on the frontier molecular orbitals of these dyes by Density Functional Theory (DFT) at the B3LYP/6-31+G(d) level support facile PICT from the D-STIF conjugated blocks to the thiophene-CA terminals (Fig. 2).

Fig. 3 shows *J–V* curves of the devices made of dyes **1–5**, **2′**, and **N719**; the corresponding photovoltaic properties are summarized in Table 2. Under AM 1.5 G illumination conditions, the device efficiencies for the **D-STIF–TCA** dyes are in the range of 5.40–6.12%. The short-circuit current densities (J_{SC}) range from 11.2 to 12.8 mA cm^{-2} (*cf.* 8.25 mA cm^{-2} for **2′** and 14.4 mA cm^{-2} for **N719**) and the open circuit voltages

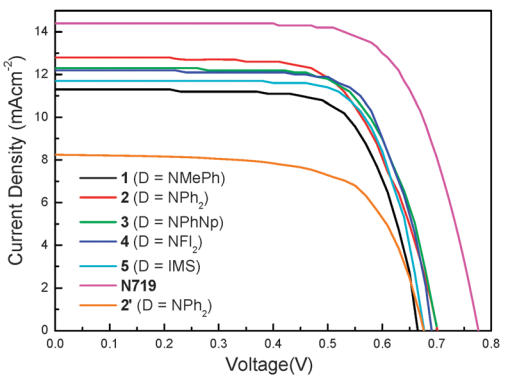

Fig. 3 Plots of photocurrent density *vs.* voltage for DSSCs based on **D-STIF–TCA** dyes **1–5**, **2′**, and **N719** under AM 1.5 G simulated solar light (100 mW cm^{-2}).

Table 1 Absorption, fluorescence and electrochemical properties of **D-STIF–TCA** and **2′** dyes

Dye	Abs., λ_{max} ($\varepsilon \times 10^{-3}$)[a]/nm	Em., λ_{max}[b]/nm	$E(S^+/S)$[c]/V	$E(S^+/S^*)$[c]/V	E_{0-0}[d]/eV
MeN-STIF–TCA (1)	375 (20.0), 452 (17.8)/442 (0.88)	622	+0.54	−1.79	2.33
PhN-STIF–TCA (2)	379 (20.1), 452 (17.1)/461 (0.64)	607	+0.63	−1.78	2.41
NpN-STIF–TCA (3)	380 (24.1), 457 (19.4)/462 (0.68)	640	+0.55	−1.82	2.37
Fl_2N-STIF–TCA (4)	374 (39.7), 492 (16.8)/476 (0.55)	615	+0.36	−2.02	2.38
IMS-STIF–TCA (5)	369 (25.2), 456 (23.1)/461 (0.65)	621	+0.52	−1.83	2.35
PhN-STB–TCA (2′)	406 (10.9)/374-435 (0.56)	467/576	+0.51	−1.87	2.38

[a] Measured in THF and on TiO_2 film. [b] Measured in THF. [c] Electrochemical data of **D-STIF–TCA** and **2′** dyes measured in DMF containing 0.1 M TBA (PF_6). Measurements were conducted by using glassy carbon as a working electrode and a Pt counter electrode with a scan rate of 100 mV s^{-1}. Potentials are quoted with reference to the internal ferrocene standard ($E_{1/2}$ = 423 mV *vs.* Ag/AgCl). [d] The band-gap, E_{0-0}, was derived from the observed optical edge.

Table 2 Photovoltaic properties of the DSSCs made of **D-STIF–TCA**, **2′** and **N719** dyes[a]

Dye	V_{OC}/mV	J_{SC}/mA cm^{-2}	FF	η (%)	DL/nmol cm^{-2}
1	677	11.2	0.71	5.40	185.7
2	705	12.8	0.66	5.96	213.8
3	702	12.3	0.70	6.04	204.5
4	697	12.2	0.72	6.12	217.5
5	680	11.7	0.73	5.83	255.9
N719	777	14.4	0.70	7.83	158.3
2′	678	8.3	0.67	3.77	284.1

[a] Measured under the standard AM 1.5 G illumination (100 mW cm^{-2}); the active area is 0.16 cm^2 and the thickness of TiO_2 films is 16 μm.

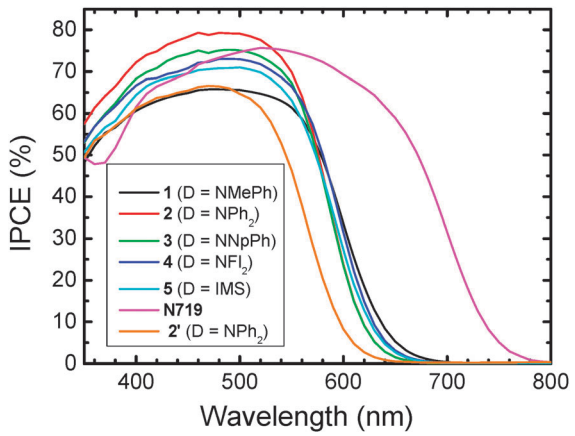

Fig. 4 The incident photon-to-current conversion efficiency stacked spectra for **D-STIF–TCA**, **2′**, and **N719** based DSSCs.

(V_{OC}) range from 677 to 705 mV (*cf.* 678 mV for **2′** and 777 mV for **N719**) and the fill factor (FF) falls in the range of 0.66–0.73 (*cf.* 0.67 for **2′** and 0.70 for **N719**). Notably, all the device performances of dyes **1–5** are 43–63% better than that of **2′** (η = 3.77%) and reached 75–78% of the **N719**-based DSSC (η = 7.83%) fabricated and measured under similar conditions.

The stacked spectra of incident photon-to-current conversion efficiency (IPCE) for devices made of **D-STIF–TCA**, **2′** and **N719** dyes are shown in Fig. 4. The band onsets of their IPCE plots fall in the range of 670–690 nm. Notably, their IPCE performances exceed 66% from 420 to 540 nm in all cases (*cf.* 53–67% for **2′** and 66–75% for **N719**) except **1** (D = NMePh; 63–66%) and exhibit the highest values (73–79%) around 490 nm (*cf.* 66% for **1** and **2′** at 490 nm). In comparison with **2**, the uniformly lower IPCE profiles from 350 to 575 nm for **1** and from 350 to 640 nm for **2′**, respectively, are responsible for their relatively smaller J_{SC} and poorer overall photovoltaic performances.

In all cases except **1** and **5**, the IPCE values are uniformly higher than those of **N719** by up to 10–20% from 350 to 490 nm. Because of the limit of light absorption, the IPCE curves of devices for **1–5** start to drop above 570 nm. The change of donor group from common NAr_2 to IMS group as in **5** led to slight erosion of its IPCE even though there exists a stronger absorption band at 455 nm as compared to those for **1–3** (Fig. 1). The amount of dye-loading (DL) of the **5**/TiO_2 film was much larger than those of the others, indicating that the degree of dye aggregation might play a role to reduce the J_{SC} of the device for **5** as compared to those of the devices for **2–4**. This interpretation is consistent with the rigidity and planar nature of the IMS group in dye **5**. Apparently, IPCE spectra show that smaller J_{SC} values of our dyes compared to that of **N719** are due to their poorer light harvesting ability in the 550–750 nm regions.

When compared with the device efficiency for **2′**, the significant improvement of the device performances by 58–62% for the spirally configured **2–4** strongly supports our molecular design concept of introducing a confined *cis*-stilbene core to reduce dye aggregation with improved conjugation and light harvesting.[12]

Notes and references

1 M. K. Nazeeruddin, A. Kay, L. Rodicio, B. R. Humphry, E. Müller, P. Liska, N. Vlachopoulos and M. Grätzel, *J. Am. Chem. Soc.*, 1993, **115**, 6382.

2 (*a*) M. Grätzel, *J. Photochem. Photobiol., A*, 2004, **164**, 3; (*b*) B. O'Reagen and M. Grätzel, *Nature*, 1991, **353**, 737.

3 (*a*) M. K. Nazeeruddin, F. DeAngelis, S. Fantacci, A. Selloni, G. Viscardi, P. Liska, S. Ito, B. Takeru and M. Grätzel, *J. Am. Chem. Soc.*, 2005, **127**, 16835; (*b*) Y. Chiba, A. Islam, Y. Watanabe, R. Komiya, N. Koide and L. Han, *Jpn. J. Appl. Phys., Part 1*, 2006, **45**, L638.

4 (*a*) H. Imahori, T. Umeyama and S. Ito, *Acc. Chem. Res.*, 2009, **42**, 1809; (*b*) M. V. Martínez-Díaz, G. de la Torrea and T. Torres, *Chem. Commun.*, 2010, **46**, 7090; (*c*) M. G. Walter, A. B. Rudine and C. C. Wamser, *J. Porphyrins Phthalocyanines*, 2010, **14**, 759.

5 (*a*) S. Kim, J. K. Lee, S. O. Kang, J. Ko, J. H. Yum, A. Fantacci, F. D. Angelis, D. Di Censo, M. K. Nazeeruddin and M. Gräzel, *J. Am. Chem. Soc.*, 2006, **128**, 16701; (*b*) M. Xu, S. Wenger, H. Bala, D. Shi, R. Li, Y. Zhou, S. M. Zakeeruddin, M. Grätzel and P. Wang, *J. Phys. Chem. C*, 2009, **113**, 2966; (*c*) H. Qin, S. Wenger, M. Xu, F. Gao, X. Jing, P. Wang, S. M. Zakeeruddin and M. Grätzel, *J. Am. Chem. Soc.*, 2008, **130**, 9202; (*d*) Y. Bai, J. Zhang, D. Zhou, Y. Wang, M. Zhang and P. Wang, *J. Am. Chem. Soc.*, 2011, **133**, 11442; (*e*) J. Liu, F. Wang, F. Fabregat-Santiago, S. G. Miralles, X. Jing, J. Bisquert and P. Wang, *J. Phys. Chem. C*, 2011, **115**, 14425.

6 (*a*) Y. I. Kim and B. A. Gregg, *J. Phys. Chem.*, 1994, **98**, 2412; (*b*) S. Erten-Ela, D. Yilmaz, B. Icli, Y. Dede, S. Icli and E. U. Akkaya, *Org. Lett.*, 2008, **10**, 3299; (*c*) Y. Shibano, T. Umeyama, Y. Matano and H. Imahori, *Org. Lett.*, 2007, **9**, 1971; (*d*) M. Miyashita, K. Sunahara, T. Nishikawa, Y. Uemura, N. Koumura, K. Hara, A. Mori, T. Abe, E. Suzuki and S. Mori, *J. Am. Chem. Soc.*, 2008, **130**, 17874; (*e*) W. Zeng, Y. Cao, Y. Bai, Y. Wang, Y. Shi, M. Zhang, F. Wang, C. Pan and P. Wang, *Chem. Mater.*, 2010, **22**, 1915.

7 (*a*) C.-T. Chen and I.-C. Chou, *J. Am. Chem. Soc.*, 2000, **122**, 7662; (*b*) C.-T. Chen, Y. Wei, J.-S. Lin, M. V. R. K. Moturu, W.-S. Chao, Y.-T. Tao and C.-H. Chien, *J. Am. Chem. Soc.*, 2006, **128**, 10992; (*c*) Y. Wei and C.-T. Chen, *J. Am. Chem. Soc.*, 2007, **129**, 7478; (*d*) Y. Wei, S. Samori, S. Tojo, M. Fujitsuka, J. S. Lin, C.-T. Chen and T. Majima, *J. Am. Chem. Soc.*, 2009, **131**, 6698; (*e*) C.-T. Chen, J.-S. Lin, M. Murthy, Y.-T. Tao and C.-H. Chiang, *Chem. Commun.*, 2005, 3980.

8 (*a*) A. Abbotto, N. Manfredi, C. Marinzi, F. De Angelis, E. Mosconi, J.-H. Yum, Z. Xianxi, M. K. Nazeeruddin and M. Grätzel, *Energy Environ. Sci.*, 2009, **2**, 1094; (*b*) S. Kolemen, O. A. Bozdemir, Y. Cakmak, G. Barin, S. Erten-Ela, M. Marszalek, J.-H. Yum, S. M. Zakeeruddin, M. K. Nazeeruddin, M. Grätzel and E. U. Akkaya, *Chem. Sci.*, 2011, **2**, 949.

9 (*a*) G. Li, K.-J. Jiang, Y.-F. Li, S.-L. Li and L.-M. Yang, *J. Phys. Chem. C*, 2008, **112**, 11591; (*b*) J. Heo, J.-W. Oh, H.-I. Ahn, S.-B. Lee, S.-E. Cho, M.-R. Kim, J.-K. Lee and N. Kim, *Synth. Met.*, 2010, **160**, 2143.

10 (*a*) S. Hwang, J. H. Lee, C. Park, H. Lee, C. Kim, C. Park, M.-H. Lee, W. Lee, J. Park, K. Kim, N.-G. Park and C. Kim, *Chem. Commun.*, 2007, 4887; (*b*) The power conversion efficiencies vary from 4.6 to 5.4% based on our own device fabrication and property measurement; (*c*) H. Zhou, P. Xue, Y. Zhang, X. Zhao, J. Jia, X. Zhang, X. Liu and R. Lu, *Tetrahedron*, 2011, **67**, 8477.

11 See ESI† for details.

12 An X-ray crystal structure (with a SQEEZE refinement) of Ph_2N-STIF–FCA indicates slight co-planarity in the confined *cis*-stilbene core in view of the dihedral angle of 22° between C=C and flanking phenyl groups[11].